ACS Pharmacology & Translational Science

pubs.acs.org/ptsci

Article

Neuroprotective Effect of Swertiamarin in a Rotenone Model of Parkinson's Disease: Role of Neuroinflammation and Alpha-Synuclein Accumulation

Monika Sharma,[‖] Fehmina Mushtaque Malim,[‖] Ashutosh Goswami,[⊥] Nishant Sharma,[⊥] Sai Sowmya Juvvalapalli, Sayan Chatterjee, Abhijeet S. Kate,[*] and Amit Khairnar[*]

Cite This: *ACS Pharmacol. Transl. Sci.* 2023, 6, 40−51

Read Online

ACCESS | Metrics & More | Article Recommendations | Supporting Information

ABSTRACT: Parkinson's disease (PD) is a progressive neurodegenerative disease with no permanent cure affecting around 1% of the population over 65. There is an urgency to search for a disease-modifying agent with fewer untoward effects. PD pathology involves the accumulation of toxic alpha-synuclein (α-syn) and neuronal inflammation leading to the degeneration of dopaminergic (DAergic) neurons. Swertiamarin (SWE), a well-studied natural product, possesses a strong anti-inflammatory effect. It is a secoiridoid glycoside isolated from *Enicostemma littorale* Blume. SWE showed a reversal effect on the α-syn accumulation in the 6-hydroxydopamine (6-OHDA)-induced *Caenorhabditis elegans* model of PD. However, there are no reports in the literature citing the effect of SWE as a neuroprotective agent in rodents. The present study aimed to evaluate the anti-inflammatory activity of SWE against lipopolysaccharide (LPS)-induced C6 glial cell activation and its neuroprotective effect in the intrastriatal rotenone mouse PD model. SWE treatment showed a significant reduction in interleukin-6 (IL-6), tumor necrosis factor-α (TNF-α), and interleukin-1β (IL-1β) levels in LPS-induced C6 glial cell activation. Further, our studies demonstrated the suppression of microglial and astroglial activation in substantia nigra (SN) after administration of SWE (100 mg/kg, intraperitoneally) in a rotenone mouse model. Moreover, SWE alleviated the rotenone-induced α-syn overexpression in the striatum and SN. SWE ameliorated the motor impairment against rotenone-induced neurotoxicity and mitigated the loss of DAergic neurons in the nigrostriatal pathway. Therefore, SWE has the potential to develop as an adjunct therapy for PD, but it warrants further mechanistic studies.

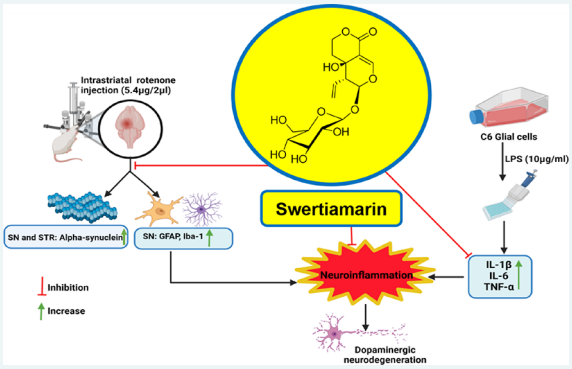

KEYWORDS: *Parkinson's disease, swertiamarin, rotenone, neuroinflammation, alpha-synuclein, dopaminergic neurodegeneration*

Parkinson's disease (PD) is characterized by the loss of dopaminergic (DAergic) neurons in the substantia nigra (SN), resulting in a decrease in dopamine (DA) levels in the striatum. It results in the development of cardinal motor symptoms such as resting tremors, rigidity, and akinesia/bradykinesia accompanied by non-motor symptoms like depression, olfactory dysfunction, sleep disorders, constipation, and cognitive decline.[1−3] The histopathological hallmark of PD is the presence of Lewy bodies in the soma and Lewy neurites in the axon terminals of DAergic neurons consisting of alpha-synuclein (α-syn).[4] Current treatment strategies are mainly symptomatic and failed to halt or slow down the evolution of PD.[5] To meet the need for disease-modifying PD drugs, a search for bioactive compounds from natural origin is warranted.

Many epidemiological studies directed toward the harmful role of inflammatory processes and microglia activation in the development of PD.[6] A significantly large number of activated microglial cells were found near the dying neurons of the SN of PD patients.[7] Pro-inflammatory cytokines such as tumor necrosis factor-α (TNF-α), interleukin-1β (IL-1β), and interleukin-6 (IL-6) were found to be upregulated in cerebrospinal fluid, serum, and brain specimens of PD patients.[8−10] Additionally, translocation of nuclear factor (NF)-kB to the nucleus has been increased in the SN of these patients, which is majorly involved in pro-inflammatory cytokine release.[11] The data of pre-clinical studies indicated that excessive activation of glial cells leads to the release of pro-inflammatory factors, nitric oxide (NO), and reactive oxygen species (ROS), showing detrimental effects on DAergic neurons.[12]

Received: June 23, 2022
Published: December 14, 2022

The specific cause of PD is still unclear. However, regular contact with environmental toxins is known to enhance the risk of developing PD.[13] Rotenone is a natural pesticide that is an inhibitor of mitochondrial complex-I. It is often used to induce PD-like pathology in animals.[14,15] *In vitro* studies with BV2 microglial cells have shown that rotenone directly induces microglial cell activation by stimulating the NF-kB signaling pathway. Moreover, the *in vivo* rotenone models showed substantial microglial activation and release of pro-inflammatory cytokines, which is the prominent mechanism behind DAergic neurodegeneration.[16−18] Rotenone causes neuroinflammation and increases α-syn levels by stimulating its de novo synthesis.[19] Therefore, we selected the rotenone model to investigate the possible therapeutic agent for reducing the DAergic neuronal cell death in PD.

Swertiamarin (SWE), a secoiridoid glycoside, has shown promising anti-inflammatory properties exhibited by various mechanisms such as NF-kB inhibition, peroxisome proliferator receptor-gamma (PPAR-γ) agonism and free radical scavenging, etc.[20−22] Recently, SWE demonstrated its neuroprotective effect in the α-syn-overexpressing transgenic and 6-hydroxydopamine (6-OHDA)-induced *Caenorhabditis elegans* models of PD.[23] However, SWE must be tested in rodent-based models to add its translational value. Therefore, we planned to investigate the neuroprotective effect of SWE against lipopolysaccharide (LPS)-induced inflammation in C6 glial cells, rotenone-induced neuroinflammation, α-syn accumulation, and DAergic neurodegeneration in a mouse model of PD.

RESULTS AND DISCUSSION

Phytochemicals from medicinal plants are tremendously reviving and extensively contributing to new drug discoveries. It is worth exploring bioactive natural products as a lead molecule to find the cure for PD. We have selected SWE, a well-reported molecule, for its potent anti-inflammatory activities, and its beneficial effects have been exhibited in the *C. elegans* model of PD.[23] Here, we report the results of *in vitro* studies, where the effect of SWE on LPS-induced C6 glial cell activation was tested. Further, the compound was administered to a rotenone mouse PD model to understand and evaluate the potential of SWE.

Large-Scale Isolation of Swertiamarin. The reported methodologies of small-scale isolation of SWE[21,24,25] were referred to, and the purification process was modified to isolate the required quantities of SWE. The process development involved solvent partitioning and precipitation steps for the enrichment of SWE, which subsequently reduced the sample load for large-scale isolation of the compound by column chromatography. The large-scale isolation was carried out in three steps, including removing polar impurities in the first step and precipitation of SWE from the mother liquor in the second step. Finally, the close-eluting compounds were separated by silica-based column chromatography. The modified extraction and purification methodology has helped isolate gram-scale quantities of SWE with desired purity, which was then used to evaluate its anti-inflammatory and neuroprotective activities in both *in vitro* and *in vivo* studies. The structure of the compound (Figure 1) was confirmed using nuclear magnetic resonance (NMR) analysis and high-resolution mass spectrometry results (Figures S2−S4). The theoretical and observed accurate mass was comparable with acceptable mass ppm error (−4.78 ppm). The observed ^{1}H and ^{13}C NMR chemical shifts followed the corresponding reported SWE values.[26,27] Further, the absolute configuration of the compound was assigned based on the obtained specific optical rotation (SOR) data, which matched the reported value.[28−30]

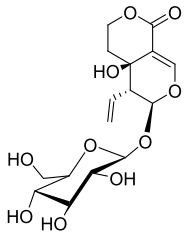

Figure 1. Structure of swertiamarin.

Anti-Inflammatory Effect of SWE on LPS-Induced C6 Glial Cell Activation. LPS, an endotoxin from Gram-negative bacteria, is extensively utilized to induce inflammation in several *in vitro* and *in vivo* PD models to understand the anti-inflammatory and neuroprotective effects of the tested compounds.[31 −33] We have incubated C6 glial cells with LPS and treated them with SWE at different concentrations selected based on cell cytotoxicity data (Figure S1). The RT-PCR data analysis of the LPS-treated cells showed significantly higher mRNA expression of cytokines IL-1β ($p < 0.01$), IL-6 ($p < 0.01$), and TNF-α ($p < 0.001$) than in untreated cells. However, SWE co-treated cells showed attenuation in pro-inflammatory cytokine mRNA expression, i.e., of IL-1β ($p < 0.05$), IL-6 ($p < 0.05$), and TNF-α ($p < 0.05$) with 25 μg/mL, of IL-1β ($p < 0.01$), IL-6 ($p < 0.05$), and TNF-α ($p < 0.01$) with 50 μg/mL and IL-1β ($p < 0.01$), IL-6 ($p < 0.01$), and TNF-α ($p < 0.01$) with 100 μg/mL (Figure 2). In a reported study, SWE was found to reduce LPS-induced activation of RAW macrophages by reducing the expression of NF-kB.[20] It suppresses the pilocarpine-induced release of pro-inflammatory cytokines (TNF-α, IL-1β, and IL-6) and inhibits astroglial cell activation in the hippocampus.[20,34−36] These shreds of evidence support the anti-inflammatory properties of SWE. It has been noted that the compounds having an anti-inflammatory effect showed neuroprotection in PD.[37−39] Therefore, we further tested the neuroprotective effect of SWE in the rotenone mouse PD model.

SWE Restored Rotenone-Induced Motor Impairment. We tested SWE in different behavioral tests by assessing motor activity, i.e., apomorphine-induced rotation, rotarod, and grip strength. An apomorphine-induced rotation test was performed on day 40 after unilateral intrastriatal (i.s.) rotenone injection to explore the effect on the rotational behavior of animals. We observed that the rotenone group animals showed a significantly greater number of contralateral turns/h ($p < 0.05$) upon apomorphine administration when compared to other groups (Figure 3A). The results indicate rotenone-induced DAergic neuronal injury in the ipsilateral region of the mouse brain. Interestingly, animals treated with rotenone and SWE both showed a significantly decrease in the number of contralateral turns/h ($p < 0.05$) as compared to the rotenone group, suggesting that SWE prevented rotenone-induced DAergic neuronal injury in the striatum (Figure 3A). However, there were no significant differences in the number of ipsilateral turns/h between all the groups (Figure 3B).

The rotarod test was carried out on days 14, 28, and 40 after the rotenone injection. We observed that latency to fall from the rod was significantly decreased (day 14, $p < 0.05$; day 28, $p < .001$; day 40, $p < 0.01$) in rotenone group animals as compared to sham animals, indicating that rotenone caused significant

https://doi.org/10.1021/acsptsci.2c00120
ACS Pharmacol. Transl. Sci. 2023, 6, 40−51

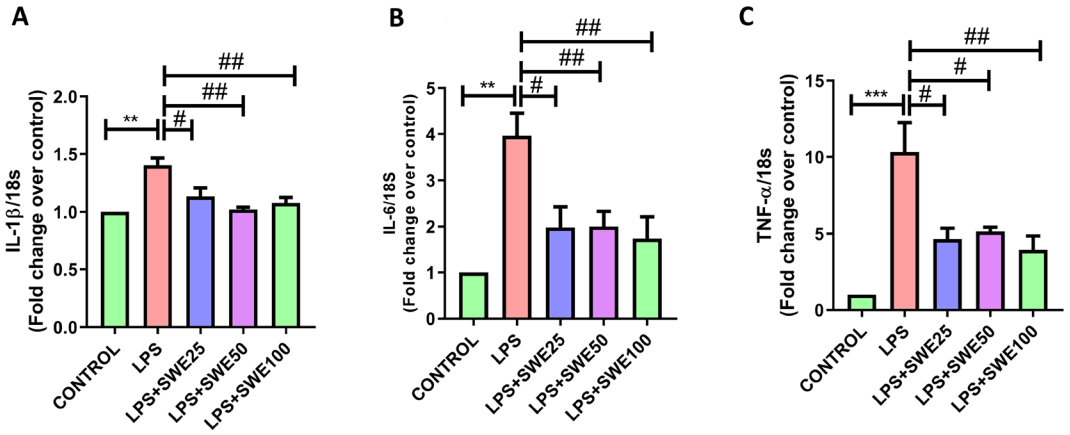

Figure 2. Effect of SWE on LPS-induced production of pro-inflammatory cytokines at 25, 50, and 100 μg/mL concentrations. This figure represents the mRNA levels of (A) IL-1β, (B) IL-6, and (C) TNF-α in C6 glial cells. Data are expressed as mean ± SEM (n = 3). Statistical significance was compared using one-way ANOVA followed by Tukey's post hoc test. **p < 0.01, ***p < 0.001 vs control; #p < 0.05, ##p < 0.01 vs LPS (10 μg/mL).

motor deficits. SWE treatment showed a marked increase in their latency to fall from the rod on day 28 (p < 0.05) and day 40 (p < 0.01) in rotenone-treated animals (Figure 3D,E). These results indicate the protective effect of SWE against rotenone-induced motor impairment. Grip strength was measured on days 14, 28, and 40 after the rotenone injection. Overall, the result displayed no significant changes in the grip strength when compared between animals from all groups, indicating that rotenone administration did not affect the muscle strength of animals (Figure 3F−H). In line with our results, a recent report highlighted that SWE improved locomotor activity in Huntington's disease by attenuating oxidative stress and improving mitochondrial enzyme activity in rats' brain regions (striatum, cortex, and hippocampus).[40]

SWE Ameliorated Rotenone-Induced Neuroinflammation in the SN of the Mouse Brain. Neuroinflammation, specifically microglial cell activation, is an essential pathological factor involved in PD. LPS-induced neurotoxicity is regionally different as LPS administration in the hippocampus, cortex, and SN leads to neurotoxicity only in the SN.[41] Later, the abundance of microglia was found to be higher in the SN compared to other regions.[41] Several anti-inflammatory agents have been tested clinically for their neuroprotective effect against PD.[37−39] Considering the anti-inflammatory effect of SWE on LPS-induced glial cell activation, we tested its anti-inflammatory effect in the rotenone mouse PD model. Rotenone, a neurotoxin, can induce neuroinflammation, causing an upsurge in glial cells in the midbrain. Immunofluorescence assays revealed that rotenone-induced significant microglial and astroglial cell activation as demonstrated by a remarkable increase in the expression of ionized calcium-binding adaptor molecule 1 (Iba-1) (p < 0.05) and glial fibrillary acidic protein (GFAP) (p < 0.01) in the SN. Although SWE has already been reported to reduce inflammation in many studies,[34,42,43] we observed for the first time that SWE inhibited microglial and astroglial cell activation in the SN of the rotenone PD model. It is evidenced by a significant decrease in Iba-1 expression (p < 0.05) (Figure 4) and GFAP expression (p < 0.05) (Figure 5) in the SN compared to the sham group.

SWE exerts anti-inflammatory effects by different mechanisms. In the case of arthritis, it is reported that SWE inhibited the release of NF-kB p65 through the JAK/STAT signaling pathway.[20] Further, its anti-inflammatory effect is reported in hepatic inflammation induced by carbon tetrachloride (CCl_4) in rats by modulating the TLR4/NF-kB signaling pathway.[35] SWE reduced the high-fat-diet-induced inflammation by suppressing the activation of the p38 mitogen-activated protein kinase (MAPK) and NF-kB pathways within the epididymal white adipose tissue (eWAT) and liver of obese mice.[44] SWE has shown anti-diabetic activity due to the upregulation of PPAR-γ,[22] a hormone nuclear receptor superfamily member responsible for modulating the immune response by inhibiting the expression of inflammatory cytokines. Importantly, agonists of PPAR-γ, such as rosiglitazone and pioglitazone, showed neuroprotection in PD as they reduced inflammation by inhibiting nuclear translocation of NF-kB.[45,46] Taken as a whole, it can be postulated that SWE could produce an anti-inflammatory effect by upregulating PPAR-γ and inhibiting nuclear translocation of NF-kB.

SWE Impedes Rotenone-Induced α-Syn Overexpression in the Midbrain. α-Syn accumulation is central to PD origin and development. Therefore, we visualized the expression of α-syn in the striatum and SN by double immunolabeling. Rotenone has been shown to cause de novo synthesis of α-syn in human neuroblastoma SH-SY5Y cells, resulting in the upregulation of α-syn expression.[19] The expression of α-syn was significantly upregulated in the striatum (p < 0.01) (Figure 6) and SN (p < 0.05) (Figure 7) of rotenone-treated animals. However, SWE treatment significantly decreased α-syn expression (p < 0.05) in the striatum (Figure 6) and SN (Figure 7) of rotenone-lesioned animals. Aiding this, a recent study by Pandey et al. demonstrated the neuroprotective effect of SWE via the increased expression of α-syn suppressive genes and stress-responsive MAPK genes in transgenic *C. elegans*, which is mediated primarily through the SKN-1/NRF-2 transcription factor.[23] As SWE has shown anti-inflammatory and α-syn lowering effects, we further tested the neuroprotective effect of SWE on DAergic neurodegeneration induced by rotenone.

SWE Ameliorated Rotenone-Induced Neurodegeneration in the Midbrain. One of the pathological hallmarks of PD is the neurodegeneration of mid-brain DAergic neurons and decreased tyrosine hydroxylase (TH) immunoreactivity. Immunohistochemistry studies indicated that rotenone administration induced a significant depletion (p < 0.01) in TH immunoreactivity in the lesioned (ipsilateral) striatum and reduction in TH^+ DAergic neurons in the SN (p < 0.05), similar to other studies, where authors found nigrostriatal degeneration after infusing intrastriatal rotenone in rats.[47−50] The co-

https://doi.org/10.1021/acsptsci.2c00120
ACS Pharmacol. Transl. Sci. 2023, 6, 40−51

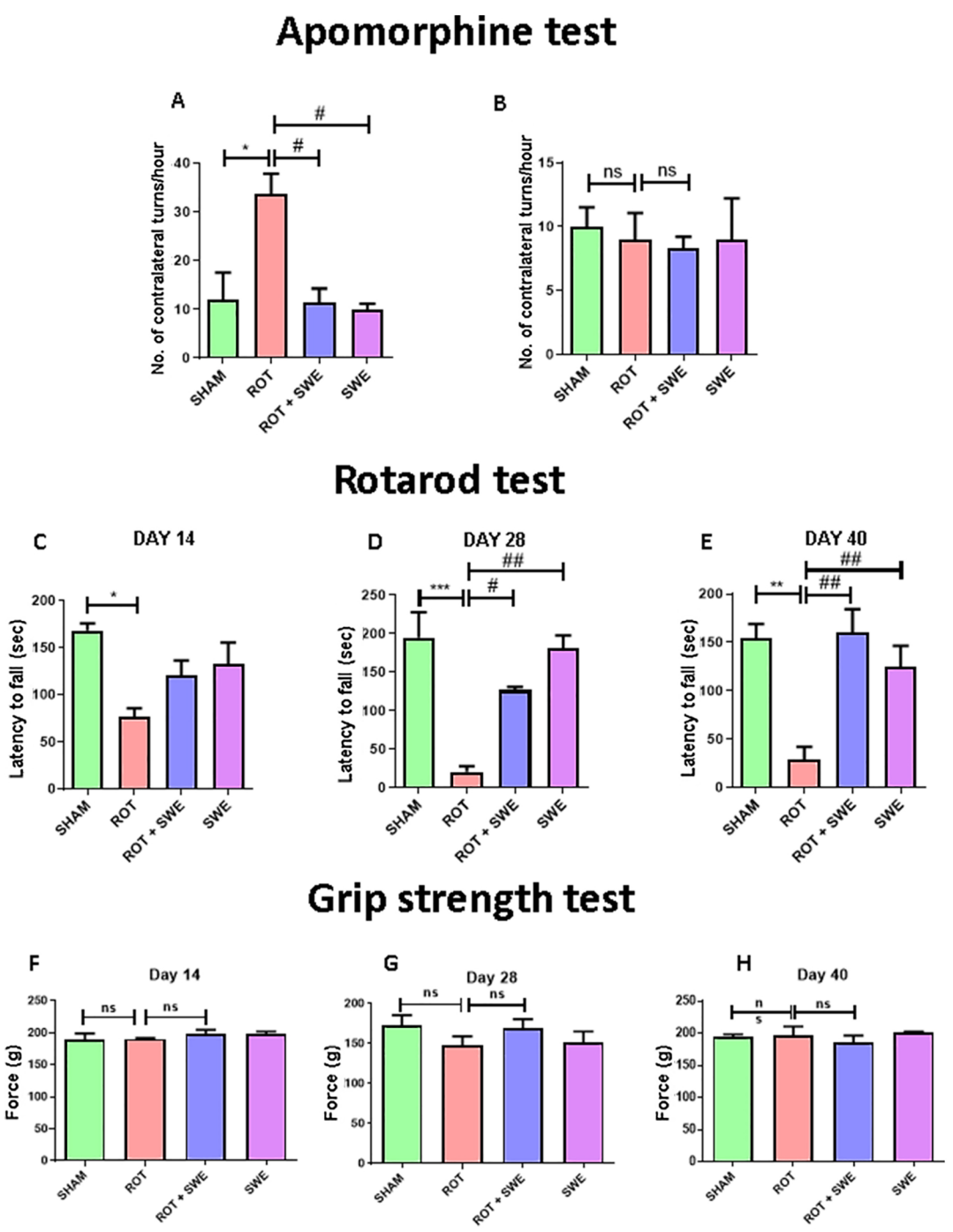

Figure 3. Effect of SWE administration on rotenone-induced motor impairment. This figure represents (A, B) the number of contralateral and ipsilateral turns per h in the apomorphine-induced rotation test, (C−E) latency to fall (s) in the rotarod test, and (F−H) force applied (in g) by mice paws to grab the grid in a grip strength test. Data are expressed as mean ± SEM ($n = 3$). Statistical significance was compared using one-way ANOVA followed by Tukey's post hoc test. *$p < 0.05$, **$p < 0.01$, ***$p < 0.001$ vs sham; #$p < 0.05$, ##$p < 0.01$ vs ROT (rotenone); ns presents no significant difference.

treatment of SWE in the rotenone mice model induced a significant increase in TH immunoreactivity in the striatum ($p < 0.05$) and an increase in the number of TH^+ neurons in SN ($p < 0.05$) (Figure 8). SWE might have provided this neuroprotection by decreasing SN neuroinflammation and reducing the α-syn accumulation in the striatum and SN.

CONCLUSIONS

The present study supports the neuroprotective potential of SWE against PD. SWE ameliorated the LPS-induced C6 glial cell activation, rotenone-induced neuroinflammation, α-syn overexpression, and DAergic neurodegeneration in mice and counteracted rotenone-induced motor impairment. Overall, SWE having a natural origin, showed protective effects in the rotenone mouse model of PD, and it needs further exploration to develop as an anti-Parkinsonian therapy.

https://doi.org/10.1021/acsptsci.2c00120
ACS Pharmacol. Transl. Sci. 2023, 6, 40−51

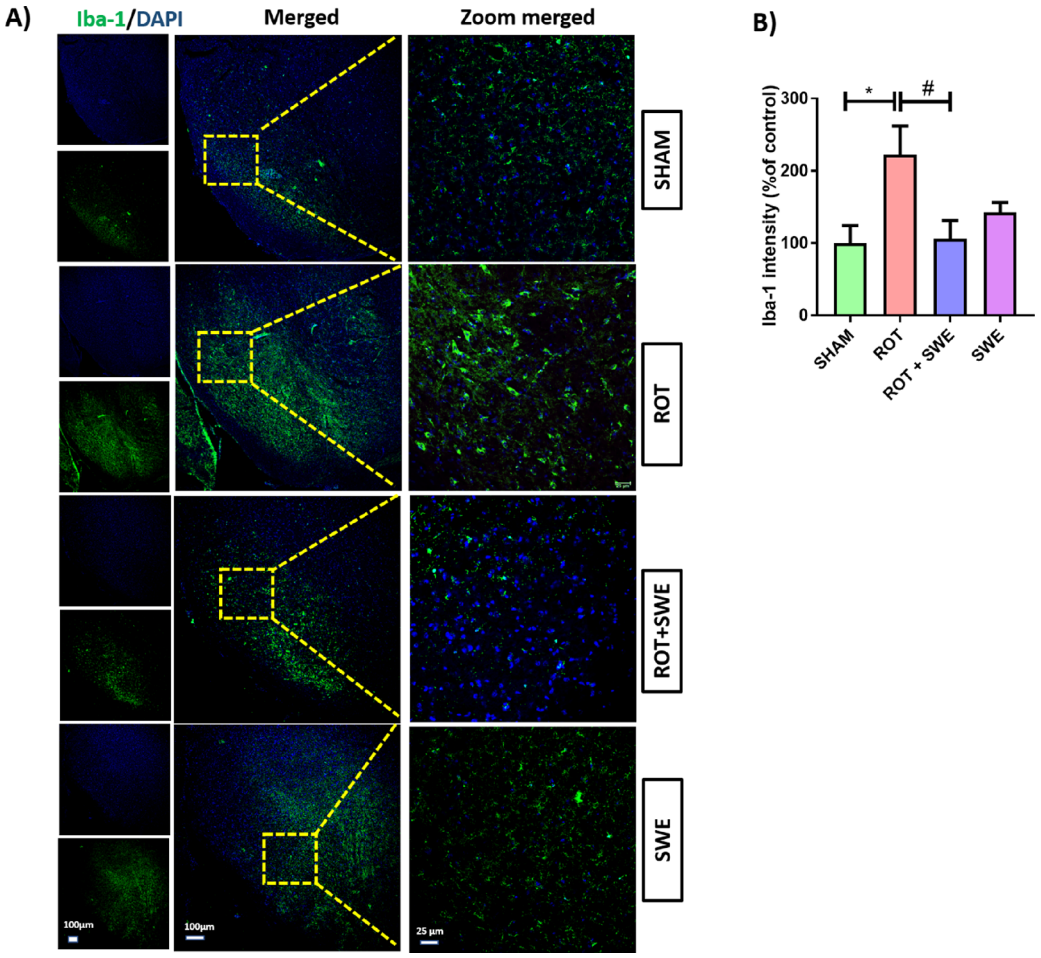

Figure 4. Effect of SWE administration on Iba-1 expression in the ipsilateral SN of rotenone-treated mice. This figure represents (A) immunofluorescence (IF) staining of Iba-1 in the SN of mice from different groups. (B) Graph representing the Iba-1 intensity (percentage of control) in the SN. Data are expressed as mean ± SEM ($n = 3$). Statistical significance was compared using one-way ANOVA followed by Tukey's post hoc test. *$p < 0.05$ vs sham; #$p < 0.05$ vs ROT (rotenone).

MATERIALS AND METHODS

Chemicals and Biologics. SWE (purity >97%, determined by HPLC) was isolated from an authentic Mamejavo powder (*Enicostemma littorale Blume*), which was procured from a retail Ayurvedic shop named Lalubhai Vrijlal Gandhi (LVG) in Ahmedabad, Gujarat (B. No. 210141). Rotenone, RNA primers (18 s, TNF-α, IL-1β, IL-6), paraformaldehyde, potassium dihydrogen phosphate, disodium hydrogen orthophosphate, resazurin, sodium chloride, potassium chloride, sodium hydroxide, Tris−HCl, trypan blue, and lipopolysaccharide (from *Escherichia coli* serotype 055:B5) were procured from Sigma-Aldrich. The solvents such as dimethyl sulfoxide, isopropyl alcohol, methanol, chloroform, and glacial acetic acid were obtained from Fisher Scientific. Absolute alcohol was obtained from Baroda Chemical Industries Pvt. Ltd., India. TRIzol reagent was purchased from Life Technologies. Components of the nutrient medium like Ham's F12 media, and fetal bovine serum (FBS), including penicillin and streptomycin, were purchased from Gibco Life Sciences. Primary and secondary antibodies were purchased from Abcam, and the Vectastain ABC Elite Kit was purchased from Vector Laboratories Limited. The cDNA synthesis kit and iTaq Universal SYBR Green Supermix were purchased from Bio-Rad.

Extraction and Isolation of SWE. The crude extract was prepared by maceration process using 1 kg of Mamejavo powder (*E. littorale Blume*) with methanol. The extract was resuspended in 1 L of water and partitioned by chloroform. Immiscible layers were separated and analyzed using thin layer chromatography (TLC) in chloroform: methanol (8.5: 1.5). The aqueous layer was lyophilized to yield a SWE-enriched fraction. Further, the lyophilized water extract (41 g) was resuspended in water and isopropyl alcohol (1: 8) and sonicated for 2 h. This step removes most of the polar impurities as sediment, and SWE remains in the mother liquor, which was concentrated by a rotary evaporator (60% volume reduction). In the concentrated solution, hexane was added in 1:3 proportion, in which SWE was precipitated. This enriched SWE fraction was purified using column chromatography by silica gel (#230−400 mesh size) stationary phase and chloroform with methanol as mobile phase. The fraction eluted at methanol: chloroform (8:92) led to the purified SWE (3.8 g). The structure of the isolated compound was confirmed by SOR, mass spectrum, and NMR data (refer to Figures S2−S4).[26,27]

HRMS (ESI$^+$): m/z calculated $[M+Na]^+$ 397.1105; observed $[M+Na]^+$ 397.1086. ^{1}H NMR (DMSO-d_6, 500 MHz): δ (ppm): 7.52 (s, 1H), 5.59 (d, $J = 1.5$ Hz, 1H), 5.38−5.36 (NR (m), 2H), 5.33 (d, $J = 5$ Hz, 1H), 5.26−5.23 (dd, $J = 5$ Hz, 7.5 Hz, 1H), 5.06 (d, $J = 5$ Hz, 1H), 5.02 (d, $J = 5.5$ Hz, 1H), 4.72 (d, $J = 2$ Hz, 1H) 4.64−4.60 (NR (m), 1H), 4.58−4.55 (m, 1H), 4.45 (d, $J =$ 8 Hz, 1H) 4.28 (m, 1H), 3.68−3.04 (m, 5H), 2.83 (m, 1H),

https://doi.org/10.1021/acsptsci.2c00120
ACS Pharmacol. Transl. Sci. 2023, 6, 40−51

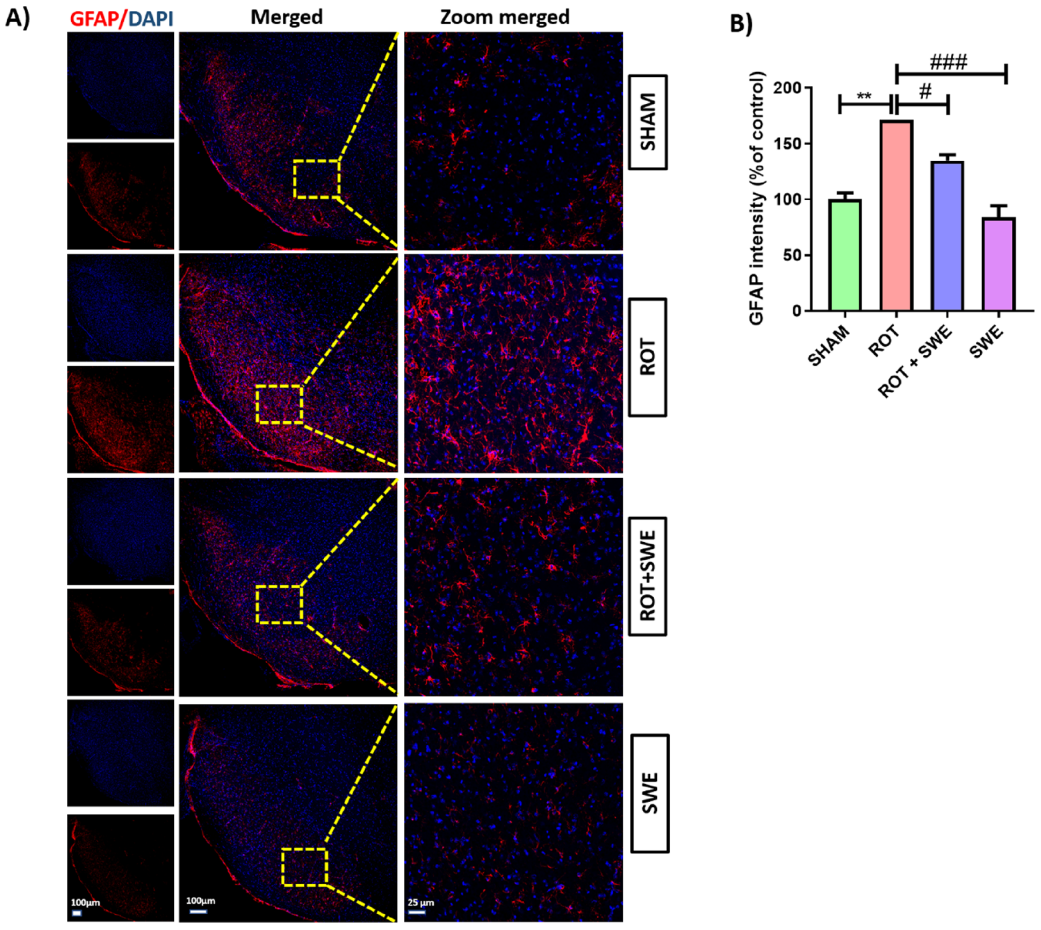

Figure 5. Effect of SWE administration on GFAP expression in the ipsilateral SN of rotenone-treated mice. This figure represents (A) IF staining of GFAP in the SN of mice from different groups. (B) Graph representing the GFAP intensity (percentage of control) in the SN. Data are expressed as mean ± SEM (n = 3). Statistical significance was compared using one-way ANOVA followed by Tukey's post hoc test. $^{**}p < 0.01$ vs sham; $\#p < 0.05$, $\#\#\#p < 0.001$ vs ROT (rotenone).

1.73−1.68 (m, 2H); ^{13}C NMR (DMSO-d_6, 125 MHz): δ (ppm): 164.5, 152.1, 133, 120.5, 108.2, 98.4, 96.5, 77.5, 76.1, 72.9, 69.9, 64.2, 62.5, 60.9, 49.9, 32.1; (NR: Not resolved). Specific optical rotation: $[\alpha]_D$ − 140.78° (c 0.25, 96% ethanol).

C6 Glial Cell Culture. The C6 glial cell line was obtained from the National Centre for Cell Science (NCCS), Pune, and cultured in vented 25 cm^2 flasks using Ham's F12 media supplemented with 10% FBS, 1% penicillin−streptomycin, and 1.5 g/L sodium bicarbonate using standard cell culture methods. The media was changed every 3 days, and the T25 flask was maintained at 37 °C in a humidified incubator (95% RH) with 5% CO_2.

Cell Viability Assay. Cells (1×10^4 cells/well) were seeded in a 96-well plate and incubated for 24 h with four different concentrations of SWE (10, 25, 50, and 100 μg/mL) dissolved in serum-free media. After incubation, Alamar blue reagent (10 μg/mL) was added per well, and the plate was incubated at 37 °C for 4 h. Fluorescence intensity was measured at 510 nm (excitation) and 590 nm (emission) wavelengths using the UV plate reader (Multiskan GO, Thermo Scientific, Finland). The fluorescence values of the untreated controls were 100%, and relative cell viability was calculated for treated concentrations.

Evaluating the Anti-Inflammatory Effect of SWE in the LPS Model of Inflammation. To determine the anti-inflammatory effect of SWE, 5×10^5 cells/well were seeded in a six-well plate and incubated for 24 h at 37 °C. After incubation, the media was discarded. The cells were treated with different concentrations of SWE (25, 50, and 100 μg/mL) dissolved in serum-free media and pre-incubated for 1 h at 37 °C. The cells were then co-treated with LPS (10 μg/mL), and the plate was incubated for 4 h. The experiment consisted of five groups: (a) untreated control, (b) LPS (10 μg/mL)-treated control, (c) LPS + SWE (25 μg/mL), (d) LPS + SWE (50 μg/mL), and (e) LPS + SWE (100 μg/mL). After completion of the incubation period, total RNA was isolated from the cells using a TRIzol reagent to evaluate the effect of SWE on the LPS-induced expression of pro-inflammatory markers by RT-PCR.

Reverse-Transcriptase Polymerase Chain Reaction. Total RNA was isolated from the cells using the TRIzol method as per the manufacturer's instructions, and purity was quantified using a Nanodrop 2000c spectrophotometer (Thermo Scientific, Wilmington, DE). Extracted RNA was reverse transcribed using a cDNA synthesis kit (Bio-Rad Laboratories, USA). The prepared cDNA was diluted using SYBR Green Supermix (Bio-Rad, USA) and primers with the Bio-Rad CFX 96 Real-Time System (Bio-Rad, USA). The TNF-α, IL-6, and Il-1β genes were quantified by the $\Delta\Delta$CT method with 18s as endogenous control. The sequence for evaluated markers is mentioned in Table 1.

Animals. Male ICR mice aged 2−3 months (35−40 g) were procured from Zydus Research Center, Ahmedabad, India, after approval from Institutional Animal Ethics Committee (IAEC),

https://doi.org/10.1021/acsptsci.2c00120
ACS Pharmacol. Transl. Sci. 2023, 6, 40−51

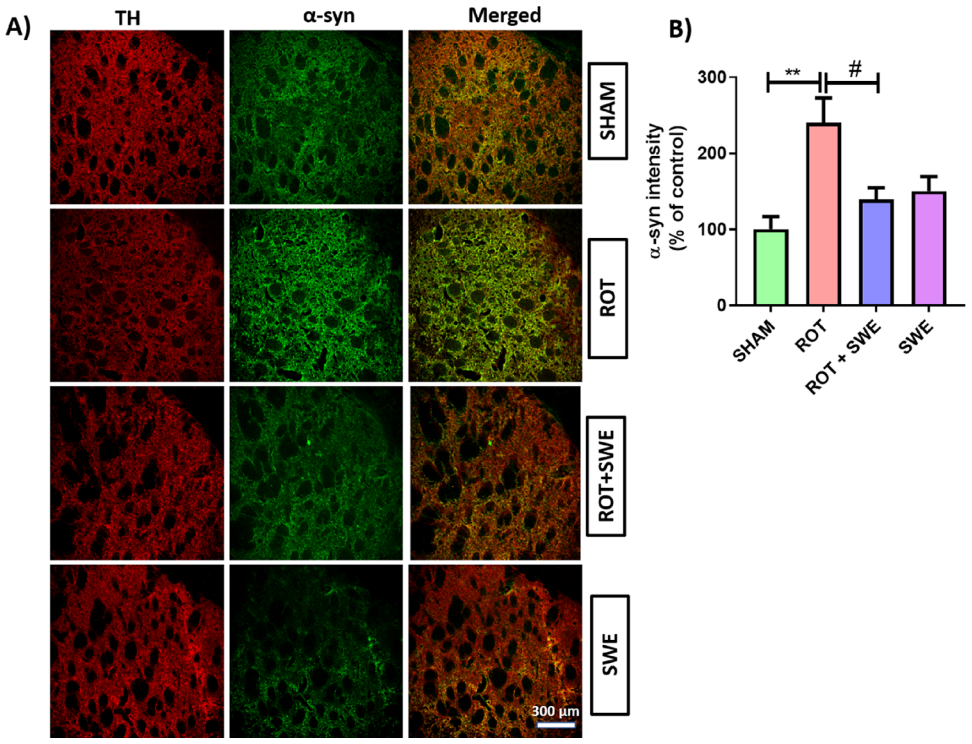

Figure 6. Effect of SWE administration on α-syn expression in ipsilateral striatum of rotenone-treated mice. This figure represents (A) IF staining of α-syn in the striatum of mice from different groups. (B) Graph representing the striatum's α-syn intensity (percentage of control). Data are expressed as mean ± SEM ($n = 3$). Statistical significance was compared using one-way ANOVA followed by Tukey's post hoc test. $^{**}p < 0.01$ vs sham; $\#p < 0.05$ vs ROT (rotenone).

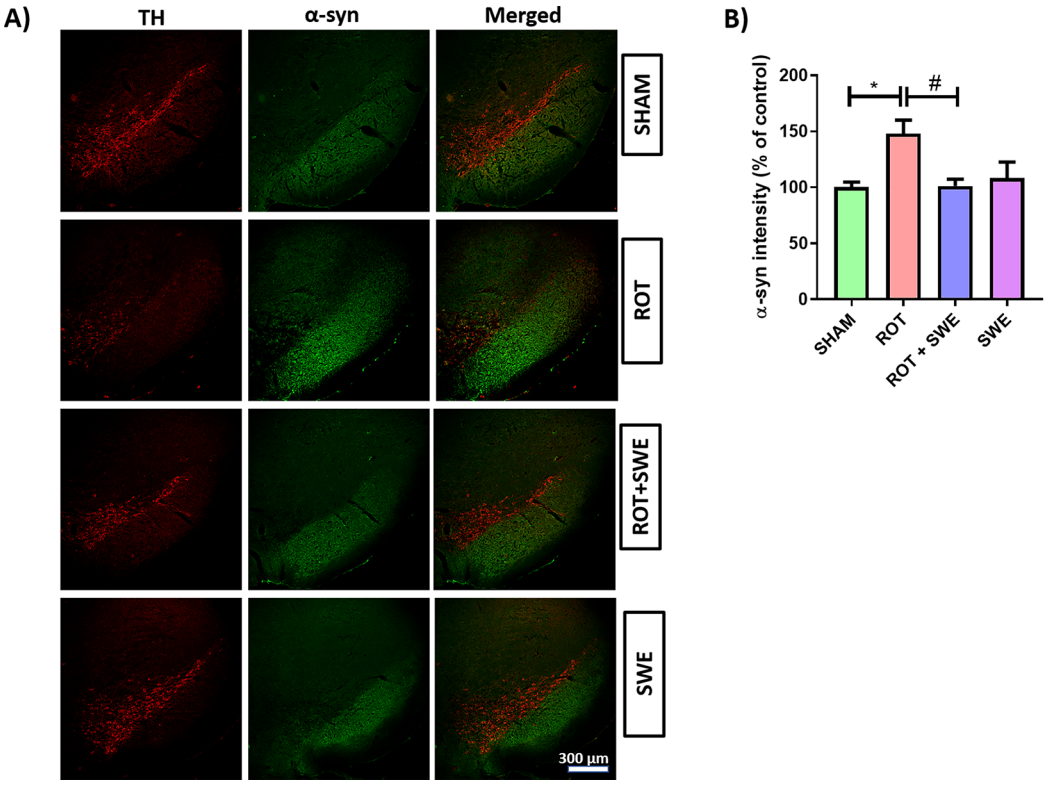

Figure 7. Effect of SWE administration on α-syn expression in the ipsilateral SN of rotenone-treated mice. This figure represents (A) IF staining of α-syn in SN of mice from different groups. (B) Graph representing the α-syn intensity (percentage of control) in the SN. Data are expressed as mean ± SEM ($n = 3$). Statistical significance was compared using one-way ANOVA followed by Tukey's post hoc test. $^{*}p < 0.05$ vs sham, $\#p < 0.05$ vs ROT (rotenone).

https://doi.org/10.1021/acsptsci.2c00120
ACS Pharmacol. Transl. Sci. 2023, 6, 40−51

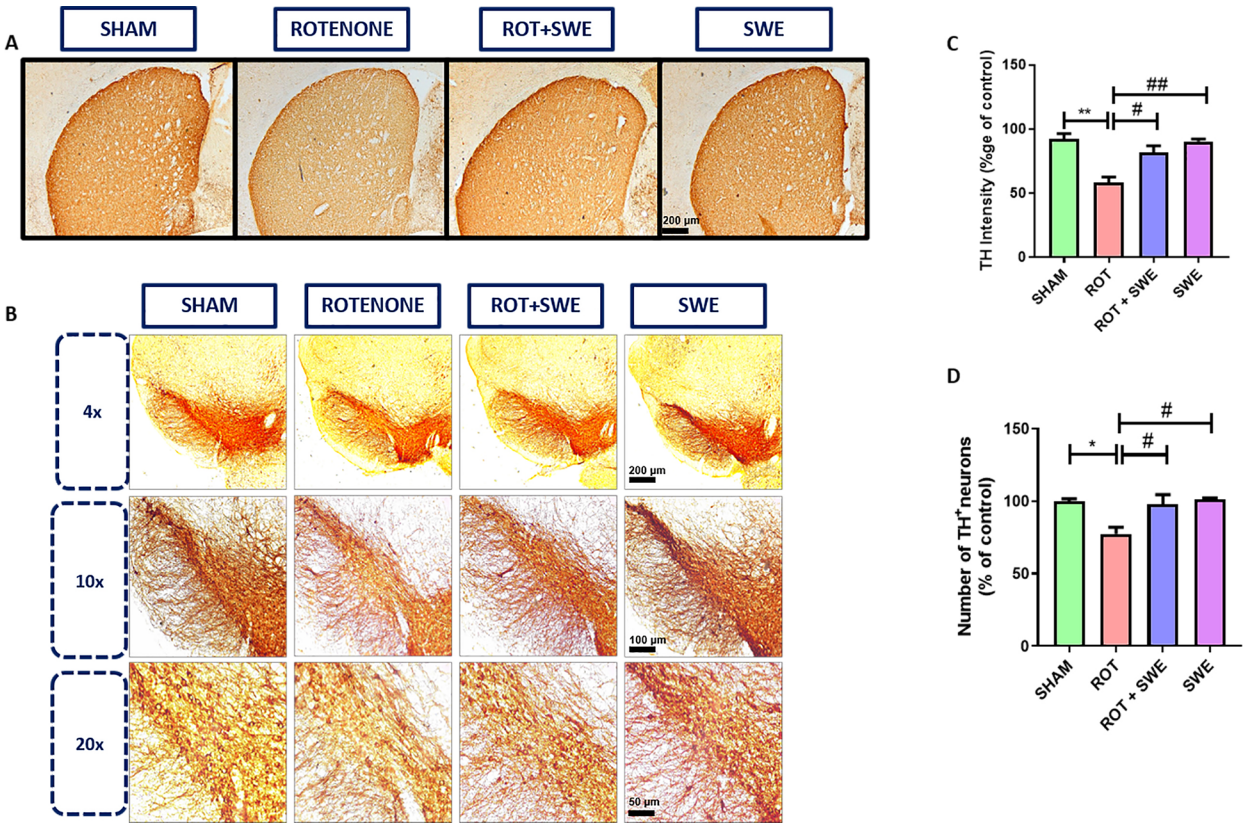

Figure 8. Effect of SWE administration on TH expression in ipsilateral striatum and number of DAergic neurons in the ipsilateral SN of rotenone-treated mice. This figure represents the immunohistochemical DAB staining of TH in the (A) striatum and (B) SN of mice from different groups. (C) Graph representing the TH intensity (percentage of control) in the striatum and (D) graph representing the number of DAergic neurons (percentage of control) in the SN. Data are expressed as mean ± SEM ($n = 3$). Statistical significance was compared using one-way ANOVA followed by Tukey's post hoc test. *$p < 0.05$, **$p < 0.01$ vs sham; #$p < 0.05$ and ##$p < 0.01$ vs ROT (rotenone).

Table 1. Primer Sequences of TNF-α, IL-6, IL-1β, and 18s

gene		sequence
TNF-α (rat)	forward	5′-ACTGAACTTCGGGGTGATTG-3′
	reverse	5′-GCTTGGTGGTTTGCTACGAC-3′
IL-6 (rat)	forward	5′-TGATGGATGCTTCCAAACTG-3′
	reverse	5′-GAGCATTGGAAGTTGGGGTA-3′
Il-1β (rat)	forward	5′-TAAGCCAACAAGTGGTATTC-3′
	reverse	5′-AGGTATAGATTCTTCCCCTTG-3′
18s	forward	5′-ATCGGGGATTGCAATTATTC-3′
	reverse	5′-CTCACTAAACCATCCAATCG-3′

NIPER-A (approval number: NIPERA/IAEC/2020/008). Animals were quarantined for 1 week in a controlled environment with relative humidity (60 ± 5%) and room temperature (25 ± 0.5 °C). A light−dark cycle of 12 h was maintained. Food and water were provided ad libitum to the animals throughout the experimental period. All the experiments were conducted as per the guidelines of the Committee for the Purpose of Control and Supervision of Experiments on Animals (CPCSEA), India. The IAEC Committee of NIPER Ahmedabad reviewed and approved all experimental methods. The mice's body weights were observed and regularly reported to check for any effect of rotenone or SWE on body weight.

Experimental Design. Animals were first divided into four different groups: Group A: sham; Group B: Rotenone (5.4 μg/2 μL DMSO); Group C: Rotenone (5.4 μg/2 μL DMSO) + SWE (100 mg/kg, i.p.); and Group D: SWE (100 mg/kg, i.p.). Group A mice were injected with intrastriatal DMSO. Group B and Group C mice were administered intrastriatal rotenone by stereotaxic surgery. For Group C and D mice, SWE treatment began 1 week before intrastriatal rotenone and DMSO injection, respectively, and continued for 40 days post-injection until sacrifice.

Rotenone was dissolved in DMSO, and SWE was solubilized in a sterile saline solution. The solutions were freshly prepared before administration. Animals were anesthetized by injecting a ketamine/xylazine cocktail (90 mg/kg ketamine and 10 mg/kg xylazine diluted with saline) intraperitoneally. The stereotaxic coordinates for the striatum, anteroposterior (AP) +0.4, mediolateral (ML) −2.0, and dorsoventral (DV) −3.3 were located, and a hole was drilled in the skull at this position using a drill bead. Rotenone solution (5.4 μg dissolved in 2 μL of DMSO) or the solvent (2 μL of DMSO) was infused directly into the right striatum of the mouse brain using a 30 gauge, 10 μL Hamilton syringe.[49] The infusion rate was maintained at 0.067 μL/min with an injection time of 30 min. The needle was allowed to stay at the injection site for 10 min post-injection to allow for adequate diffusion of the solution. The post-operative care was provided until the full recovery of the animals.

Behavioral studies were performed on day −7 (before SWE pretreatment) and days 7, 14, 28, and 40 of the study. On day 41, after injection, all animals were sacrificed by transcardial perfusion with 4% buffered PFA. The ipsilateral brain hemispheres were removed and stored at 4 °C in 4% PFA for use in future experiments (Figure 9).

https://doi.org/10.1021/acsptsci.2c00120
ACS Pharmacol. Transl. Sci. 2023, 6, 40−51

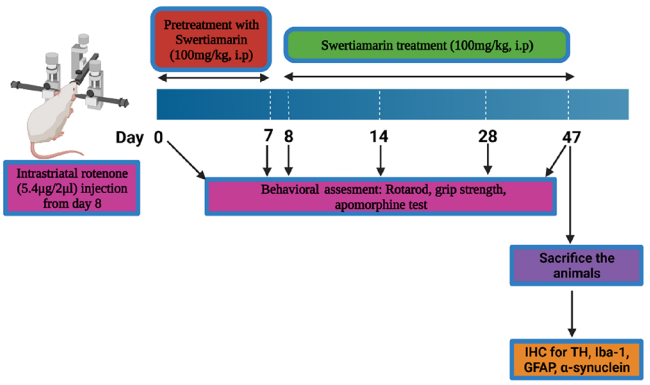

Figure 9. Schematic representation of the experimental design.

Behavioral Assessment for Model Validation and Motor Impairment. *Apomorphine-Induced Rotation Test.* This test was performed with minor modifications to monitor the motor impairment caused by the unilateral striatal lesion.[51] Mice were placed in wide glass cylinders individually and allowed to habituate for 10 min. Apomorphine (0.5 mg/kg, s.c.) was administered subsequently, and mice were placed back into the cylinders. After 10 min, the number of complete (360^0) turns in either the ipsilateral (lesion side) or contralateral (the side opposite to the lesion) direction was recorded for 60 min.

Rotarod Test. A rotarod apparatus (Harvard apparatus) assessed the motor coordination of mice.[52] All animals were trained to walk on the rotating rod at a constant speed of 4 rpm for 3 days. After training, the final test was carried out in an acceleration mode (2 to 20 rpm for 300 s). Each animal was tested three times with 30 min intervals, and the time taken by the animal to fall from the rod was recorded. The average of three trials was considered for statistical analysis.

Grip Strength Test. A grip strength test was performed to evaluate the muscle strength of mice using a grip strength apparatus according to the protocol mentioned by Sharma et al.[53]

Immunofluorescence Staining and Analysis. Immunofluorescence staining for α-syn and TH was done on coronal sections of SN and striatum and for GFAP and Iba-1 on coronal sections of SN as per the protocol mentioned by Sharma et al. with little modifications.[53] The primary antibodies used were anti-TH (rabbit pAb, AB152, 1:500), anti-α-syn (mouse mAb, AB1903, 1:500), anti-GFAP (rabbit pAb, AB7260, 1:1000), and anti-Iba-1 (goat pAb, PA5-18039, 1:500). Goat pAb secondary to the mouse, Alexa-Fluor 488 (ab150113) (1:1000) and goat pAb secondary to the rabbit, Alexa-Fluor 647 (ab150079) (1:1000), donkey pAb secondary to goat, Alexa-Fluor 555 (ab150134) were used as the fluorescent secondary antibodies. The mean fluorescence values of α-syn, Iba-1 and GFAP were measured for all three levels in the SN using ImageJ software (version 1.42, NIH, USA).[54] Background measures were also taken for each section and subtracted from the mean fluorescence values, and the corrected values were presented as a percentage of control (sham taken as control).

Immunohistochemistry: DAB Staining. The ipsilateral brain hemispheres fixed in 4% buffered PFA overnight were treated with 15% sucrose solution (prepared in PBS, pH 7.4) followed by 30% sucrose solution at 4 °C for 24 h each. The brains were cut into 40 μm coronal sections at three different levels for SN (−3.52, −3.16, and −2.92 mm) and striatum (1.10, 0.74, and 0.38 mm) using a cryostat (Thermo Scientific) and DAB staining, and section mounting was performed as per the protocol used by Sharma et al.[53] Images were then acquired using a Leica DMi1 inverted microscope.

Quantitative Analysis of DAB Staining. Image analysis was done using ImageJ software [National Institutes of Health (NIH), Bethesda, MD, USA] as mentioned in previous literature.[55−57] Extent of immunostaining of TH^+ fibers in the striatum was presented as a percentage of optical density (OD) in sham/control mice. ImageJ was first calibrated using the Rodbard function within the software to normalize the grayscale range (0−255) into OD values. Each image was transformed into 8 bit (grayscale). The OD values were then normalized by eliminating the OD values of the background. It was done for all three levels of the striatum, and then we calculated the average of these levels. The average values of all the groups were normalized concerning control (sham) values.

The number of DAergic neurons was calculated as described by Sharma et al.[53] and presented as a percentage of the control (sham) group.

Data Analysis. GraphPad Prism 5.0 Software (San Diego, CA, USA) was used to analyze data. Data were presented as mean ± standard error mean (SEM). The analysis of raw data was performed using a one-way analysis of variance and then applying post hoc Tukey's test for comparison between different treatment groups. $p < 0.05$ was considered statistically significant.

■ ASSOCIATED CONTENT

Supporting Information

The Supporting Information is available free of charge at https://pubs.acs.org/doi/10.1021/acsptsci.2c00120.

Alamar assay, +ESI-MS mass spectrum, ^{1}H and ^{13}C NMR details of SWE, and body weights of animals (PDF)

■ AUTHOR INFORMATION

Corresponding Authors

Abhijeet S. Kate − *Department of Natural Products, National Institute of Pharmaceutical Education and Research (NIPER), Ahmedabad, Gujarat 382355, India*; Phone: +79 66745555; Email: kate.abhi.s@gmail.com, abhijeetk@niperahm.ac.in

Amit Khairnar − *Department of Pharmacology and Toxicology, National Institute of Pharmaceutical Education and Research (NIPER), Ahmedabad, Gujarat 382355, India; International Clinical Research Center, St. Anne's University Hospital Brno, Brno 656 91, Czech Republic;* orcid.org/0000-0003-3375-774X; Phone: +91 9284349396; Email: amitkhairnar520@gmail.com.

Authors

Monika Sharma − *Department of Pharmacology and Toxicology, National Institute of Pharmaceutical Education and Research (NIPER), Ahmedabad, Gujarat 382355, India*

Fehmina Mushtaque Malim − *Department of Pharmacology and Toxicology, National Institute of Pharmaceutical Education and Research (NIPER), Ahmedabad, Gujarat 382355, India*

Ashutosh Goswami − *Department of Natural Products, National Institute of Pharmaceutical Education and Research (NIPER), Ahmedabad, Gujarat 382355, India*

Nishant Sharma − *Department of Pharmacology and Toxicology, National Institute of Pharmaceutical Education and Research (NIPER), Ahmedabad, Gujarat 382355, India*

https://doi.org/10.1021/acsptsci.2c00120
ACS Pharmacol. Transl. Sci. 2023, 6, 40−51

Sai Sowmya Juvvalapalli − *Department of Natural Products, National Institute of Pharmaceutical Education and Research (NIPER), Ahmedabad, Gujarat 382355, India*
Sayan Chatterjee − *Department of Pharmacology and Toxicology, National Institute of Pharmaceutical Education and Research (NIPER), Ahmedabad, Gujarat 382355, India*

Complete contact information is available at: https://pubs.acs.org/10.1021/acsptsci.2c00120

Author Contributions

[⊥]A.G. and N.S. have contributed equally to this work.

Author Contributions

[‖]M.S. and F.M.M. have contributed equally to this work.

Author Contributions

We declare that all authors made fundamental contributions to the manuscript. A.M.K. and A.K. designed the study. M.S., F.M.M., S.S.J., and A.G. conducted experiments. A.M.K., A.K., M.S., F.M.M., A.G., N.S., and S.C. analyzed the data. A.M.K., A.K., M.S., F.M.M., A.G., N.S., and S.C. participated in the interpretation and writing of the manuscript. All authors read and approved the final manuscript.

Funding

This supplement was supported by the National Institute of Pharmaceutical Education and Research (NIPER) seed fund Ahmedabad, Department of Pharmaceutics, Ministry of Chemicals and Fertilizers, Government of India. A.K. gratefully acknowledges the support of the Ramalingaswami Fellowship from the Department of Biotechnology, India.

Notes

The authors declare no competing financial interest.
No clinical study was conducted. The IAEC approved the experimental design for the pre-clinical study of NIPER Ahmedabad (IAEC approval number: NIPERA/IAEC/2020/008).

■ ACKNOWLEDGMENTS

The authors acknowledge the National Institute of Pharmaceutical Education and Research (NIPER) Ahmedabad administration for providing the facility and support for conducting this study. They were supported by project no. LX22NPO5107 (MEYS) and financed by European Union − Next Generation EU.

■ LIST OF ABBREVIATIONS

α-syn	alpha-synuclein
ANOVA	analysis of variance
AP	anteroposterior
cDNA	complementary DNA
CPCSEA	Committee for the Purpose of Control and Supervision of Experiments on Animals
DA	dopamine
DAB	3,3′-diaminobenzidine
DAergic	dopaminergic
DAPI	4′,6- diamidino-2-phenylindole
DMSO	dimethyl sulfoxide
DNA	deoxyribonucleic acid
DPX	dibutylphthalate polystyrene xylene
DV	dorsoventral
FBS	fetal bovine serum
GFAP	glial fibrillary acidic protein
i.p.	intraperitoneal
IAEC	Institutional Animal Ethics Committee
Iba-1	ionized calcium-binding adaptor molecule 1
ICR	institute of Cancer Research
IL-1β	interleukin-1 beta
IL-6	interleukin-6
L-DOPA	levo- 3,4-dihydroxyphenylalanine
LPS	lipopolysaccharides
MAPK	mitogen-activated protein kinase
ML	mediolateral
mRNA	messenger ribonucleic acid
NCCS	National Centre for Cell Science
NF-κB	nuclear factor kappa light chain enhancer of activated B cells
NMR	nuclear magnetic resonance
OD	optical density
6-OHDA	6-hydroxydopamine
PBS	phosphate-buffered saline
PD	Parkinson's disease
PFA	paraformaldehyde
qRT-PCR	quantitative reverse transcription−polymerase chain reaction
RH	relative humidity
RNA	ribonucleic acid
Rpm	revolutions per minute
s.c.	subcutaneous
SEM	standard error of the mean
SN	substantia nigra
SWE	swertiamarin
TH	tyrosine hydroxylase
TNF- α	tumor necrosis factor- α
UV	ultraviolet

■ REFERENCES

(1) Gokcal, E.; Gur, V. E.; Selvitop, R.; Yildiz, G. B.; Asil, T. Motor and non-motor symptoms in Parkinson's disease: effects on quality of life. *Arch. Neuropsychiatry* **2017**, *54*, 143−149.
(2) Amara, A. W.; Memon, A. A. Effects of exercise on non-motor symptoms in Parkinson's disease. *Clin. Ther.* **2018**, *40*, 8−15.
(3) Chan, C. S.; Guzman, J. N.; Ilijic, E.; Mercer, J. N.; Rick, C.; Tkatch, T.; Meredith, G. E.; Surmeier, D. J. Rejuvenation'protects neurons in mouse models of Parkinson's disease. *Nature* **2007**, *447*, 1081−1086.
(4) Gómez-Benito, M.; Granado, N.; García-Sanz, P.; Michel, A.; Dumoulin, M.; Moratalla, R. Modeling Parkinson's disease with the alpha-synuclein protein. *Front. Pharmacol.* **2020**, *11*, 356.
(5) Rizek, P.; Kumar, N.; Jog, M. S. An update on the diagnosis and treatment of Parkinson disease. *Cmaj* **2016**, *188*, 1157−1165.
(6) McGeer, P. L.; McGeer, E. G. Inflammation and neurodegeneration in Parkinson's disease. *Parkinsonism Relat. Disord.* **2004**, *10*, S3−S7.
(7) McGeer, P. L.; McGeer, E. G. Glial reactions in Parkinson's disease. *Mov. Disord.* **2008**, *23*, 474−483.
(8) Hirsch, E. C.; Hunot, S. Neuroinflammation in Parkinson's disease: a target for neuroprotection? *Lancet Neurol.* **2009**, *8*, 382−397.
(9) Blum-Degena, D.; Müller, T.; Kuhn, W.; Gerlach, M.; Przuntek, H.; Riederer, P. Interleukin-1β and interleukin-6 are elevated in the cerebrospinal fluid of Alzheimer's and de novo Parkinson's disease patients. *Neurosci. Lett.* **1995**, *202*, 17−20.
(10) Dobbs, R.; Charlett, A.; Purkiss, A.; Dobbs, S.; Weller, C.; Peterson, D. Association of circulating TNF-α and IL-6 with ageing and parkinsonism. *Acta Neurol. Scand.* **1999**, *100*, 34−41.
(11) Hunot, S.; Brugg, B.; Ricard, D.; Michel, P. P.; Muriel, M.-P.; Ruberg, M.; Faucheux, B. A.; Agid, Y.; Hirsch, E. C. Nuclear translocation of NF-κB is increased in dopaminergic neurons of patients with Parkinson disease. *Proc. Natl. Acad. Sci.* **1997**, *94*, 7531−7536.

(12) Domingues, A. V.; Pereira, I. M.; Vilaça-Faria, H.; Salgado, A. J.; Rodrigues, A. J.; Teixeira, F. G. Glial cells in Parkinson' s disease: protective or deleterious? *Cell. Mol. Life Sci.* **2020**, 1−18.
(13) Goldman, S. M. Environmental toxins and Parkinson's disease. *Annu. Rev. Pharmacol. Toxicol.* **2014**, *54*, 141−164.
(14) Sherer, T. B.; Kim, J.-H.; Betarbet, R.; Greenamyre, J. T. Subcutaneous rotenone exposure causes highly selective dopaminergic degeneration and α-synuclein aggregation. *Exp. Neurol.* **2003**, *179*, 9−16.
(15) Betarbet, R.; Sherer, T. B.; MacKenzie, G.; Garcia-Osuna, M.; Panov, A. V.; Greenamyre, J. T. Chronic systemic pesticide exposure reproduces features of Parkinson's disease. *Nat. Neurosci.* **2000**, *3*, 1301−1306.
(16) Gao, H.-M.; Hong, J.-S.; Zhang, W.; Liu, B. Distinct role for microglia in rotenone-induced degeneration of dopaminergic neurons. *J. Neurosci.* **2002**, *22*, 782−790.
(17) Gao, H.-M.; Liu, B.; Hong, J.-S. Critical role for microglial NADPH oxidase in rotenone-induced degeneration of dopaminergic neurons. *J. Neurosci.* **2003**, *23*, 6181−6187.
(18) Sherer, T. B.; Betarbet, R.; Kim, J.-H.; Greenamyre, J. T. Selective microglial activation in the rat rotenone model of Parkinson's disease. *Neurosci. Lett.* **2003**, *341*, 87−90.
(19) Sala, G.; Arosio, A.; Stefanoni, G.; Melchionda, L.; Riva, C.; Marinig, D.; Brighina, L.; Ferrarese, C. Rotenone upregulates alpha-synuclein and myocyte enhancer factor 2D independently from lysosomal degradation inhibition. *BioMed Res. Int.* **2013**, *2013*, 1.
(20) Saravanan, S.; Islam, V. H.; Babu, N. P.; Pandikumar, P.; Thirugnanasambantham, K.; Chellappandian, M.; Raj, C. S. D.; Paulraj, M. G.; Ignacimuthu, S. Swertiamarin attenuates inflammation mediators via modulating NF-κB/I κB and JAK2/STAT3 transcription factors in adjuvant induced arthritis. *Eur. J. Pharm. Sci.* **2014**, *56*, 70−86.
(21) Vaijanathappa, J.; Badami, S. Antiedematogenic and free radical scavenging activity of swertiamarin isolated from Enicostemma axillare. *Planta Med.* **2009**, *75*, 12−17.
(22) Vaidya, H.; Goyal, R. K.; Cheema, S. K. Anti-diabetic activity of swertiamarin is due to an active metabolite, gentianine, that upregulates PPAR-γ gene expression in 3T3-L1 cells. *Phytother. Res.* **2013**, *27*, 624−627.
(23) Pandey, T.; Shukla, A.; Trivedi, M.; Khan, F.; Pandey, R. Swertiamarin from Enicostemma littorale, counteracts PD associated neurotoxicity via enhancement α-synuclein suppressive genes and SKN-1/NRF-2 activation through MAPK pathway. *Bioorg. Chem.* **2021**, *108*, 104655.
(24) Vishwakarma, S.; Rajani, M.; Bagul, M.; Goyal, R. A rapid method for the isolation of swertiamarin from Enicostemma littorale. *Pharm. Biol.* **2004**, *42*, 400−403.
(25) Jaishree, V.; Badami, S.; Kumar, M. R.; Tamizhmani, T. Antinociceptive activity of swertiamarin isolated from Enicostemma axillare. *Phytomedicine* **2009**, *16*, 227−232.
(26) Rana, V. Separation and identification of swertiamarin from Enicostema axillare Lam. Raynal by centrifugal partition chromatography and nuclear magnetic resonance-Mass Spectrometry. *J. Pharm Sci. Emerg. Drugs* **2014**, *1*, 2.
(27) Li, Z.; Welbeck, E.; Yang, L.; He, C.; Hu, H.; Song, M.; Bi, K.; Wang, Z. A quantitative 1H nuclear magnetic resonance (qHNMR) method for assessing the purity of iridoids and secoiridoids. *Fitoterapia* **2015**, *100*, 187−194.
(28) Bhattacharya, S.; Reddy, P.; Ghosal, S.; Singh, A.; Sharma, P. Chemical constituents of gentianaceae XIX: CNS-depressant effects of swertiamarin. *J. Pharm. Sci.* **1976**, *65*, 1547−1549.
(29) Wang, H.; Wei, W.; Lan, X.; Liu, N.; Li, Y.; Ma, H.; Sun, T.; Peng, X.; Zhuang, C.; Yu, J. Neuroprotective effect of swertiamain on cerebral ischemia/reperfusion injury by inducing the Nrf2 protective pathway. *ACS Chem. Neurosci.* **2019**, *10*, 2276−2286.
(30) Fadzil, N. S. M.; Sekar, M.; Gan, S. H.; Bonam, S. R.; Wu, Y. S.; Vaijanathappa, J.; Ravi, S.; Lum, P. T.; Dhadde, S. B. Chemistry, Pharmacology and Therapeutic Potential of Swertiamarin−A Promising Natural Lead for New Drug Discovery and Development. *Drug Des., Dev. Ther.* **2021**, *15*, 2721.
(31) Zhou, H.-F.; Liu, X.-Y.; Niu, D.-B.; Li, F.-Q.; He, Q.-H.; Wang, X.-M. Triptolide protects dopaminergic neurons from inflammation-mediated damage induced by Lipopolysaccharide intranigral injection. *Neurobiol. Dis.* **2005**, *18*, 441−449.
(32) Tai, W.; Ye, X.; Bao, X.; Zhao, B.; Wang, X.; Zhang, D. Inhibition of Src tyrosine kinase activity by squamosamide derivative FLZ attenuates neuroinflammation in both in vivo and in vitro Parkinson's disease models. *Neuropharmacology* **2013**, *75*, 201−212.
(33) Hoban, D. B.; Connaughton, E.; Connaughton, C.; Hogan, G.; Thornton, C.; Mulcahy, P.; Moloney, T. C.; Dowd, E. Further characterisation of the LPS model of Parkinson's disease: a comparison of intra-nigral and intra-striatal lipopolysaccharide administration on motor function, microgliosis and nigrostriatal neurodegeneration in the rat. *Brain, Behav., Immun.* **2013**, *27*, 91−100.
(34) Zhang, M.; Ma, X.; Xu, H.; Wu, W.; He, X.; Wang, X.; Jiang, M.; Hou, Y.; Bai, G. A natural AKT inhibitor swertiamarin targets AKT-PH domain, inhibits downstream signaling, and alleviates inflammation. *FEBS J.* **2020**, *287*, 1816−1829.
(35) Wu, T.; Zhang, Q.; Song, H. Swertiamarin attenuates carbon tetrachloride (CCl4)-induced liver injury and inflammation in rats by regulating the TLR4 signaling pathway. *Braz. J. Pharm. Sci.* **2018**, *54*, 54.
(36) Deng, X.-H.; Zhang, X.; Wang, J.; Ma, P.-S.; Ma, L.; Niu, Y.; Sun, T.; Zhou, R.; Yu, J.-Q. Anticonvulsant effect of Swertiamarin against Pilocarpine-induced seizures in adult male mice. *Neurochem. Res.* **2017**, *42*, 3103−3113.
(37) Lee, K. M.; Lee, Y.; Chun, H. J.; Kim, A. H.; Kim, J. Y.; Lee, J. Y.; Ishigami, A.; Lee, J. Neuroprotective and anti-inflammatory effects of morin in a murine model of Parkinson's disease. *J. Neurosci. Res.* **2016**, *94*, 865−878.
(38) Ghosh, A.; Kanthasamy, A.; Joseph, J.; Anantharam, V.; Srivastava, P.; Dranka, B. P.; Kalyanaraman, B.; Kanthasamy, A. G. Anti-inflammatory and neuroprotective effects of an orally active apocynin derivative in pre-clinical models of Parkinson's disease. *J. Neuroinflammation* **2012**, *9*, 1−16.
(39) Leonoudakis, D.; Rane, A.; Angeli, S.; Lithgow, G. J.; Andersen, J. K.; Chinta, S. J. Anti-inflammatory and neuroprotective role of natural product securinine in activated glial cells: implications for Parkinson's disease. *Mediators Inflammation* **2017**, *2017*, 1.
(40) Rahul PG, R. W. Sameer SS, To Study the Effect of Swertiamarin in Animal Model of Huntington's Disease. *J. Pharm. Res.* **2018**, *2*, 1−8.
(41) Kim, W.-G.; Mohney, R. P.; Wilson, B.; Jeohn, G.-H.; Liu, B.; Hong, J.-S. Regional difference in susceptibility to lipopolysaccharide-induced neurotoxicity in the rat brain: role of microglia. *J. Neurosci.* **2000**, *20*, 6309−6316.
(42) Cafaro, T.; Carnicelli, V.; Caprioli, G.; Maggi, F.; Celenza, G.; Perilli, M.; Bozzi, A.; Amicosante, G.; Brisdelli, F. Anti-apoptotic and anti-inflammatory activity of Gentiana lutea root extract. *Adv. Tradit. Med.* **2020**, *20*, 619−630.
(43) Xiang, Y.; Haixia, W.; Zenggen, L.; Yanduo, T. Anti-inflammatory activity of compounds isolated from Swertia mussotii. *Nat. Prod. Res.* **2019**, *33*, 598−601.
(44) Xu, L.; Li, D.; Zhu, Y.; Cai, S.; Liang, X.; Tang, Y.; Jin, S.; Ding, C. Swertiamarin supplementation prevents obesity-related chronic inflammation and insulin resistance in mice fed a high-fat diet. *Adipocyte* **2021**, *10*, 160−173.
(45) Carta, A.; Frau, L.; Pisanu, A.; Wardas, J.; Spiga, S.; Carboni, E. Rosiglitazone decreases peroxisome proliferator receptor-gamma levels in microglia and inhibits TNF-alpha production: new evidences on neuroprotection in a progressive Parkinson's disease model. *Neuroscience* **2011**, *194*, 250−261.
(46) Chaturvedi, R. K.; Beal, M. F. PPAR: a therapeutic target in Parkinson's disease. *J. Neurochem.* **2008**, *106*, 506−518.
(47) Mulcahy, P.; Walsh, S.; Paucard, A.; Rea, K.; Dowd, E. Characterisation of a novel model of Parkinson's disease by intra-striatal infusion of the pesticide rotenone. *Neuroscience* **2011**, *181*, 234−242.
(48) Carriere, C.; Kang, N.; Niles, L. Neuroprotection by valproic acid in an intrastriatal rotenone model of Parkinson's disease. *Neuroscience* **2014**, *267*, 114−121.

https://doi.org/10.1021/acsptsci.2c00120
ACS Pharmacol. Transl. Sci. 2023, 6, 40−51

(49) Perez-Pardo, P.; Dodiya, H. B.; Broersen, L. M.; Douna, H.; van Wijk, N.; Lopes da Silva, S.; Garssen, J.; Keshavarzian, A.; Kraneveld, A. D. Gut−brain and brain−gut axis in Parkinson's disease models: effects of a uridine and fish oil diet. *Nutr. Neurosci.* **2018**, *21*, 391−402.
(50) Maniyath, S. P.; Solaiappan, N.; Rathinasamy, M. Neuro-behavioural changes in a hemiparkinsonian rat model induced by rotenone. *J. Clin. Diagn. Res.* **2017**, *11*, AF01.
(51) Grealish, S.; Mattsson, B.; Draxler, P.; Björklund, A. Characterisation of behavioural and neurodegenerative changes induced by intranigral 6-hydroxydopamine lesions in a mouse model of Parkinson's disease. *Eur. J. Neurosci.* **2010**, *31*, 2266−2278.
(52) Shiotsuki, H.; Yoshimi, K.; Shimo, Y.; Funayama, M.; Takamatsu, Y.; Ikeda, K.; Takahashi, R.; Kitazawa, S.; Hattori, N. A rotarod test for evaluation of motor skill learning. *J. Neurosci. Methods* **2010**, *189*, 180−185.
(53) Sharma, M.; Kaur, J.; Rakshe, S.; Sharma, N.; Khunt, D.; Khairnar, A. Intranasal Exposure to Low-Dose Rotenone Induced Alpha-Synuclein Accumulation and Parkinson's Like Symptoms Without Loss of Dopaminergic Neurons. *Neurotoxic. Res.* **2022**, *40*, 215−229.
(54) Farrand, A. Q.; Verner, R. S.; McGuire, R. M.; Helke, K. L.; Hinson, V. K.; Boger, H. A. Differential effects of vagus nerve stimulation paradigms guide clinical development for Parkinson's disease. *Brain Stimul.* **2020**, *13*, 1323−1332.
(55) Jewett, M.; Jimenez-Ferrer, I.; Swanberg, M. Astrocytic expression of GSTA4 is associated to dopaminergic neuroprotection in a rat 6-OHDA model of Parkinson's disease. *Brain Sci.* **2017**, *7*, 73.
(56) Wang, S.-j.; Wang, Q.; Ma, J.; Yu, P.-h.; Wang, Z.-m.; Wang, B. Effect of moxibustion on mTOR-mediated autophagy in rotenone-induced Parkinson's disease model rats. *Neural Regener. Res.* **2018**, *13*, 112.
(57) Xavier, L. L.; Viola, G. G.; Ferraz, A. C.; Da Cunha, C.; Deonizio, J. M. D.; Netto, C. A.; Achaval, M. A simple and fast densitometric method for the analysis of tyrosine hydroxylase immunoreactivity in the substantia nigra pars compacta and in the ventral tegmental area. *Brain Res. Protoc.* **2005**, *16*, 58−64.

https://doi.org/10.1021/acsptsci.2c00120
ACS Pharmacol. Transl. Sci. 2023, 6, 40−51